Asteroseismology of OB stars

from birth to adulthood

Peter De Cat

Royal Observatory of Belgium, Ringlaan 3, B-1180 Brussels, Belgium

... a very incomplete point of view

OB-type stars

Convective core
Radiative envelope

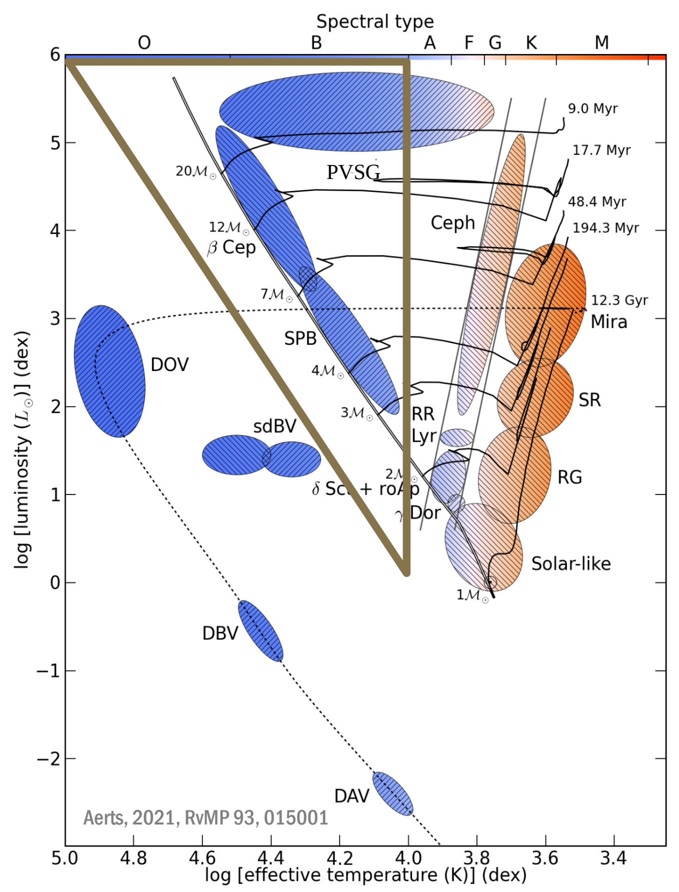

- → **β Cephei stars** (βCep)
  - ➢ Low order p and g modes with periods of few hours
- → **Slowly Pulsating B stars** (SPB)
  - ➢ High order g modes with periods of several hours to few days

} Hybrids?

- → **Periodic Variable Supergiants** (PVSG)
  - ➢ g modes with periods of order of 10 to 100 days
- → **Be stars** (Be)
  - ➢ Rotational modulation and/or Pulsations?
- → **Maia variables**
  - → Talk Handler: "Maia variables - fact or fiction?"

Excitation mechanisms at play

- ➢ Opacity mechanism operating in Z bump

Asteroseismic requirements and tools

→ Time series

→ Observed pulsation modes

- Frequency *f* ⟶ Frequency analysis
- Degree *l*
- Azimuthal number *m*

(Degree *l* and Azimuthal number *m*) ⟶ Mode identification

* Multicolour photometry: method of photometric amplitude ratios and frequency shifts (Dupret et al., 2003, A&A 398, 677)

* High-resolution spectroscopy: moment method (Aerts, 1992, A&A 266, 294; Briquet & Aerts, 2003, A&A 398, 687)

fourier parameter fit method (Zima, 2006, A&A 455, 227)

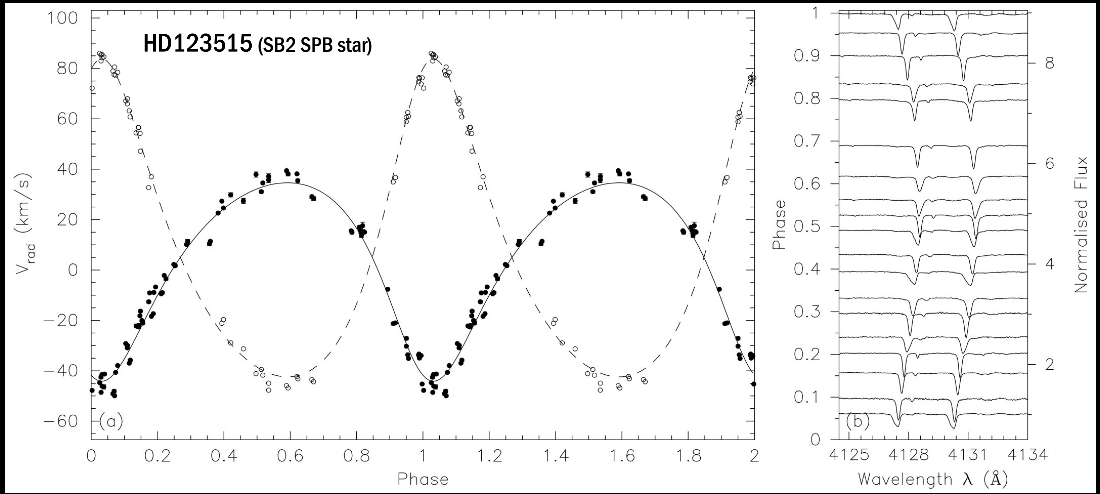

De Cat et al., 2000, A&A 355, 1015

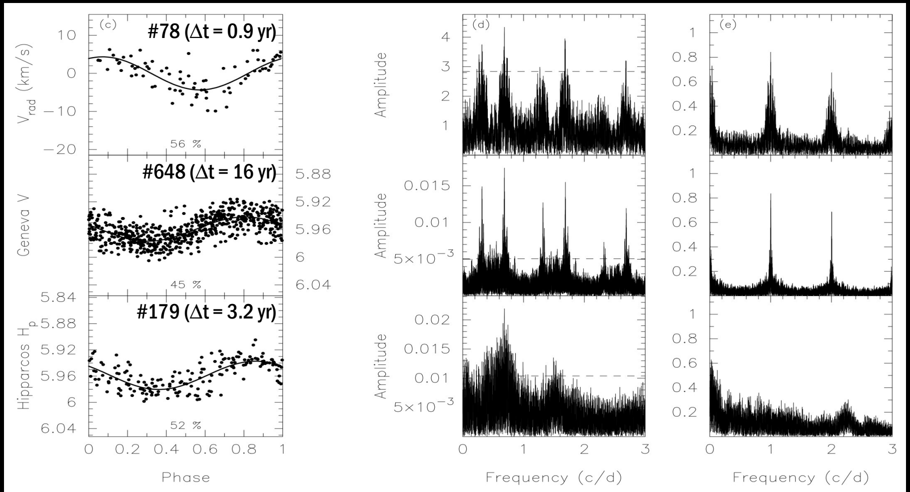

Peter De Cat (Royal Observatory of Belgium, Ringlaan 3, B-1180 Brussels, Belgium)

Asteroseismic requirements and tools

→ Time series

→ Observed pulsation modes

- Frequency f → Frequency analysis
- Degree l
- Azimuthal number m

(Degree l and Azimuthal number m) → Mode identification

* Multicolour photometry: method of photometric amplitude ratios and frequency shifts (Dupret et al., 2003, A&A 398, 677)

* High-resolution spectroscopy: moment method (Aerts, 1992, A&A 266, 294; Briquet & Aerts, 2003, A&A 398, 687)

fourier parameter fit method (Zima, 2006, A&A 455, 227)

Asteroseismic requirements and tools

→ Time series

→ Observed pulsation modes

- Frequency f ⟶ Frequency analysis
- Degree l
- Azimuthal number m

} ⟶ Mode identification

* Multicolour photometry: method of photometric amplitude ratios and frequency shifts (Dupret et al., 2003, A&A 398, 677)

* High-resolution spectroscopy: moment method (Aerts, 1992, A&A 266, 294; Briquet & Aerts, 2003, A&A 398, 687)

fourier parameter fit method (Zima, 2006, A&A 455, 227)

→ Present day asteroseismic diagnostics

- Rotational multiplets

Bowman, 2020, FrASS 7, 70

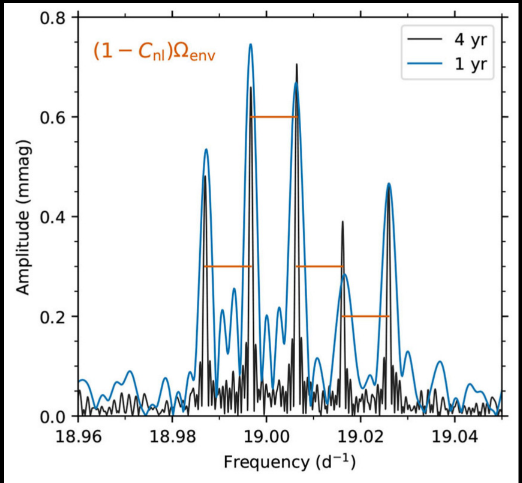

- g mode period spacing patterns (asymptotic regime)

Bowman, 2020, FrASS 7, 70

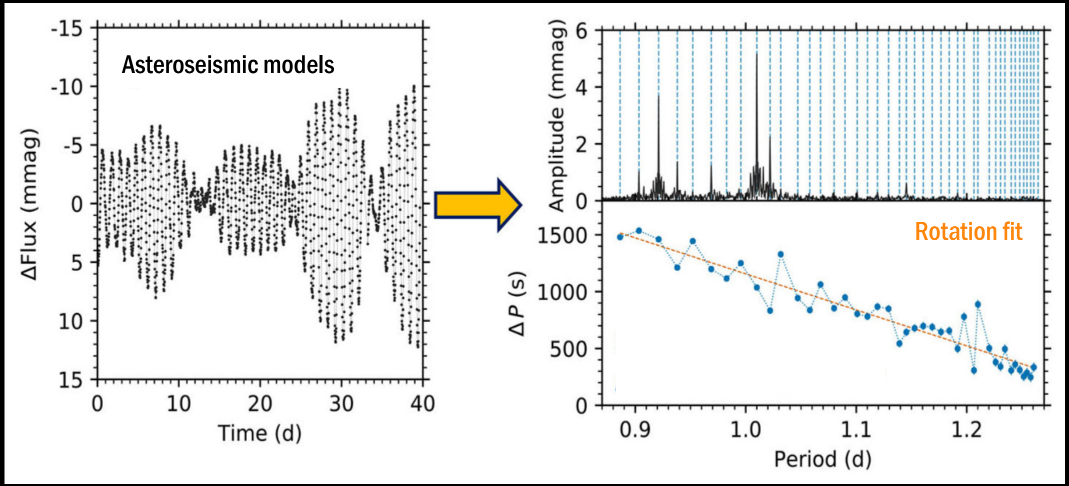

Asteroseismic requirements and tools

→ Time series

→ Observed pulsation modes

- Frequency f → Frequency analysis
- Degree l
- Azimuthal number m } → Mode identification

Poster 16 Shitrit: "Asteroseismology of Massive Stars - A Path to Population Samples"

* Multicolour photometry: method of photometric amplitude ratios and frequency shifts (Dupret et al., 2003, A&A 398, 677)
* High-resolution spectroscopy: moment method (Aerts, 1992, A&A 266, 294; Briquet & Aerts, 2003, A&A 398, 687)
  fourier parameter fit method (Zima, 2006, A&A 455, 227)

→ Present day asteroseismic diagnostics

- Rotational multiplets
- g mode period spacing patterns (asymptotic regime)

Bowman, 2020, FrASS 7, 70

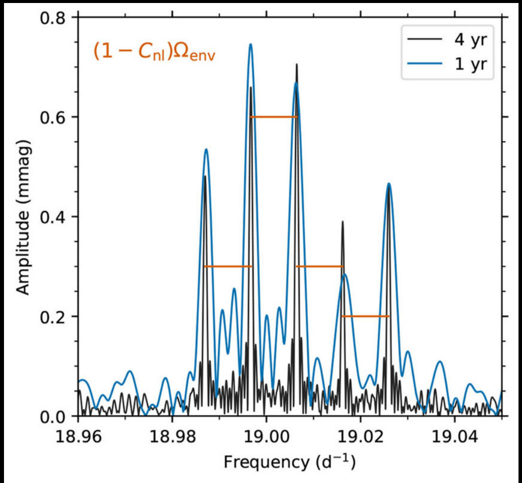

Bowman, 2020, FrASS 7, 70

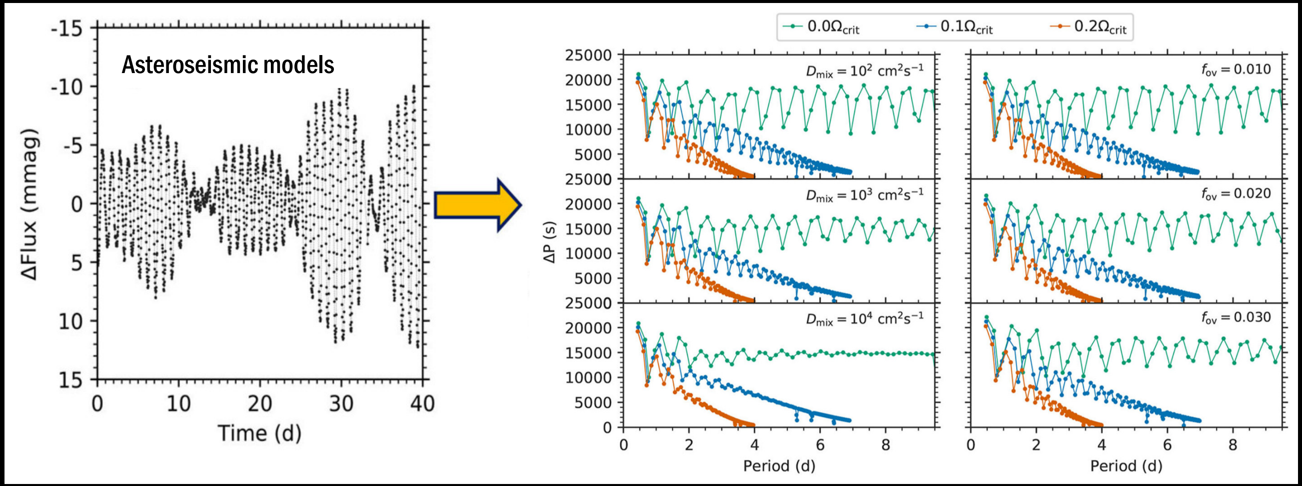

Opacities

→ KIC3240411 (Szewczuk & Daszyńska-Daszkiewicz, 2018, MNRAS 478)

- Hot hybrid B-type pulsator
- Different period spacings observed in asymptotic g-mode regime
- Seismic modelling and mode identification for series b ⟹ $(l,m) = (1,0)$
  - ✔ Effects of rotation included via the traditional approximation

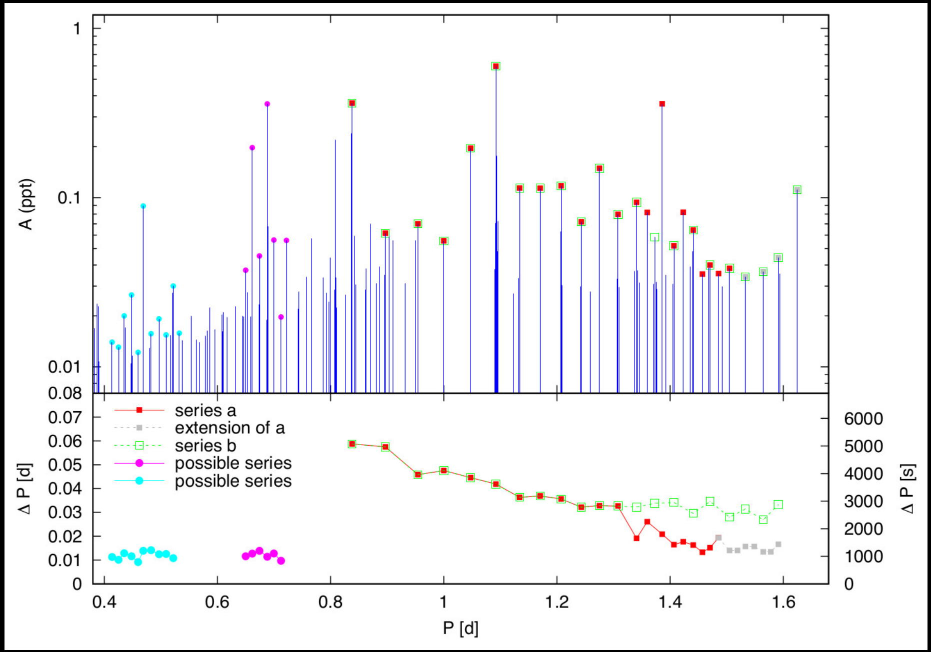

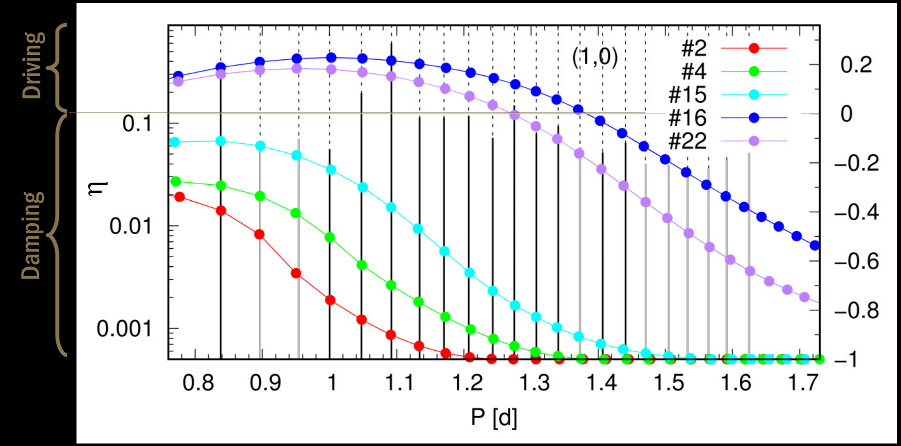

- Standard opacity models
  - ✔ #2: hydrogen abundance and metallicity as measured in photosphere (X = 0.67 and Z = 0.006)
  - ✔ #4: solar abundances cf. Asplund et al. (2009) (X = 0.738 and Z = 0.013)
- Modified opacity models
  - ✔ #15: increased opacity by 100% at log T = 5.06, 5.30 and 5.46
  - ✔ #16: substantially increased opacities at log T = 5.46
  - ✔ #22: substantially increased opacities at log T = 5.46 + minor modification at log T = 5.06 and 5.22

Opacity increase needed to excite g-modes

Talk Walczak: “KIC 8264293 - detailed study of the differential rotation”

Interior mixing profile

→ Pedersen et al., 2021, NatAs 5, 715

- Sample of 26 SPB stars showing period spacings patterns from dipole g-modes (~4% of all B stars in the nominal Kepler field of view)
- Asteroseismic modelling with eight different interior mixing profiles $D_{mix}(r)$ each having three regions (convective core $D_{conv}(r)$, core boundary layer $D_{cbl}(r)$, radiative envelope $D_{env}(r)$)

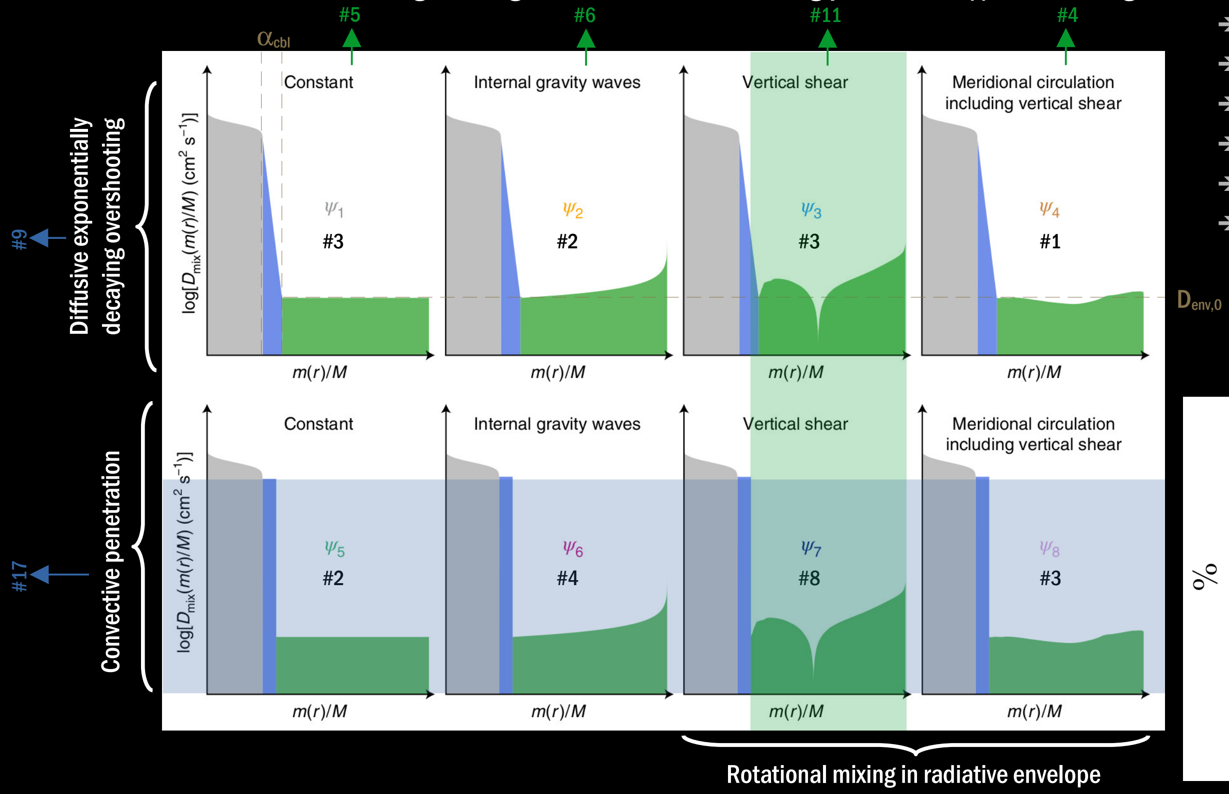

- ➔ M_{ini} initial mass
- ➔ Z metal mass fraction
- ➔ X_c/X_{ini} hydrogen mass fraction in fully mixed convective core/inital hydrogen mass fraction
- ➔ Ω_{rot} interior rotation frequency
- ➔ α_{cbl} length scale connected with the size of the core boundary layer
- ➔ $D_{env,0}$ level of mixing at bottom of radiative envelope

Majority for convective penetration (55%) vertical shear (39%)

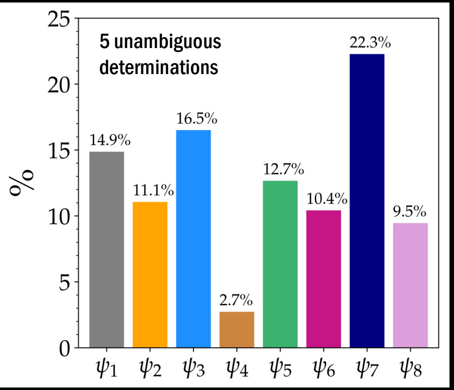

Pedersen, 2022, AJ 930, 94

➔ Expected helium core masses at end of main-sequence evolution:
* underestimated without mixing
* increase with initial stellar mass
* heavily influenced by amount of envelope mixing

cf. Kaiser et al, 2020, MNRAS 496, 1967
Johnston, 2021, A&A 655, A29

Interior mixing profile

Mass discrepancy for ecipsing binaries with convective core

- Dynamical mass ⟶ model-independent
  - ✔ Accurate masses
  - ✔ Accurate radii

  from orbital motion

- Evolutionary mass ⟶ model-dependent
  - ✔ Same age
  - ✔ Same initial composition

  in stellar interior structure and evolution (SSE) model

  from isochrone fitting of both components in Kiel diagram (T_{eff} vs. log g)

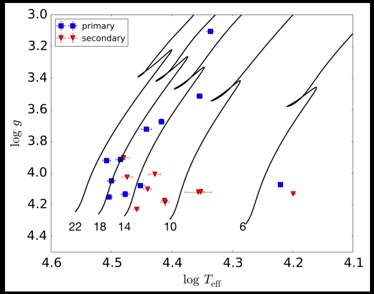

⟶ Tkachenko et al., 2020, A&A 637, A60

- Sample of 11 eclipsing SB2 sytems (fundemental and atmospheric parameters determined with same methodology)

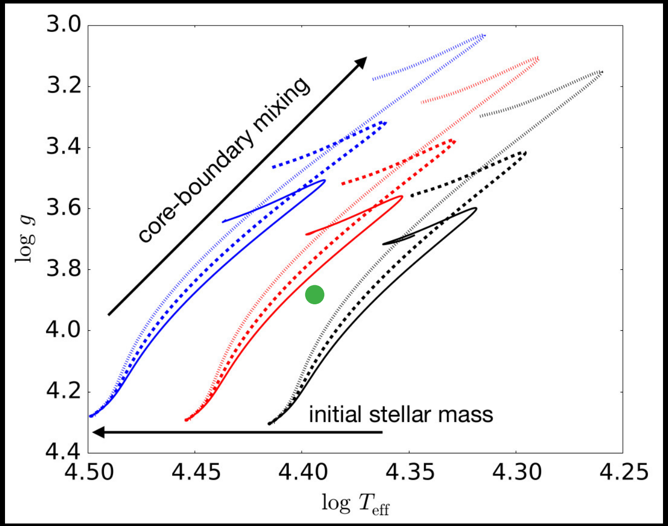

- (1) Single evolution – (2) Binary evolution (forced to have same age)
  - ✔ Reference model solution: dynamical mass, f_{ov} = 0.005
  - ✔ Initial mass solution: free mass, f_{ov} = 0.005
  - ✔ Core boundary solution: dynamical mass, f_{ov} free (max. 0.040)
  - ✔ Intial mass-core boundary solution: free mass, f_{ov} free (max. 0.040)

Interior mixing profile

Mass discrepancy for ecipsing binaries with convective core

- Dynamical mass ⟶ model-independent
  - ✔ Accurate masses
  - ✔ Accurate radii
  - from orbital motion
- Evolutionary mass ⟶ model-dependent
  - ✔ Same age
  - ✔ Same initial composition
  - in stellar interior structure and evolution (SSE) model
  - from isochrone fitting of both components in Kiel diagram (T_{eff} vs. log g)

⟶ Tkachenko et al., 2020, A&A 637, A60

- Sample of 11 eclipsing SB2 sytems (fundemental and atmospheric parameters determined with same methodology)

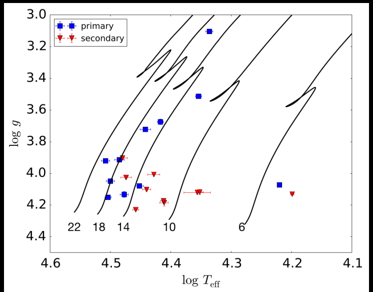

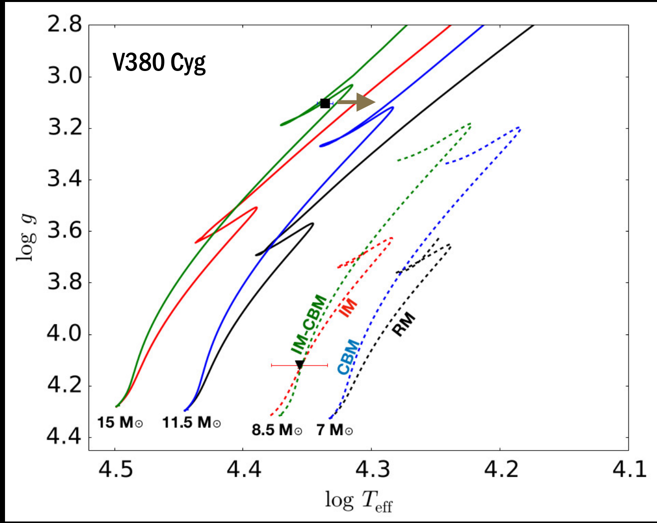

- (1) Single evolution – (2) Binary evolution (forced to have same age)
  - ✔ Reference model solution: dynamical mass, f_{ov} = 0.005
  - ✔ Initial mass solution: free mass, f_{ov} = 0.005
  - ✔ Core boundary solution: dynamical mass, f_{ov} free (max. 0.040)
  - ✔ Intial mass-core boundary solution: free mass, f_{ov} free (max. 0.040)

Mass discrepancy anti-correlated with surface gravity

(1) Convective core mass-stellar age correlation in SSE models

(2) Neglect of high microturbulent velocities and turbulent pressure in stellar atmosphere models

Ijspeert et al., 2021, A&A 652, A120: An all-sky sample of OBA-type eclipsing binaries observed by TESS

Southworth & Bowman, 2022, MNRAS 513, 3191: High-mass pulsaors in eclipsing binaries observed using TESS

Interior rotation profile

→ Pedersen, 2022, ApJ 940, 49

- 52 SPB stars for which
  - ✔ Internal rotation frequencies derived using g-mode oscillations
  - ✔ Unambiguous mode identification for at least one g-mode
  - ✔ Ages from X_c/X_{ini}, t/t_{MS} and/or log g

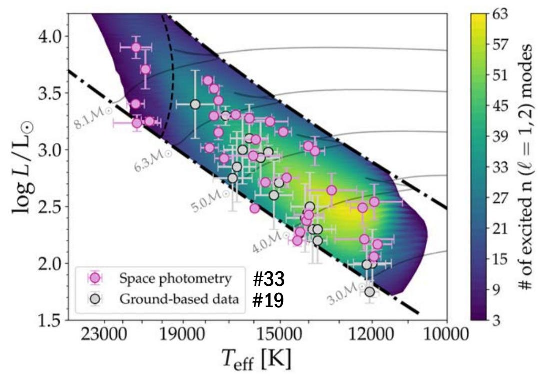

- Core rotation decreases with age

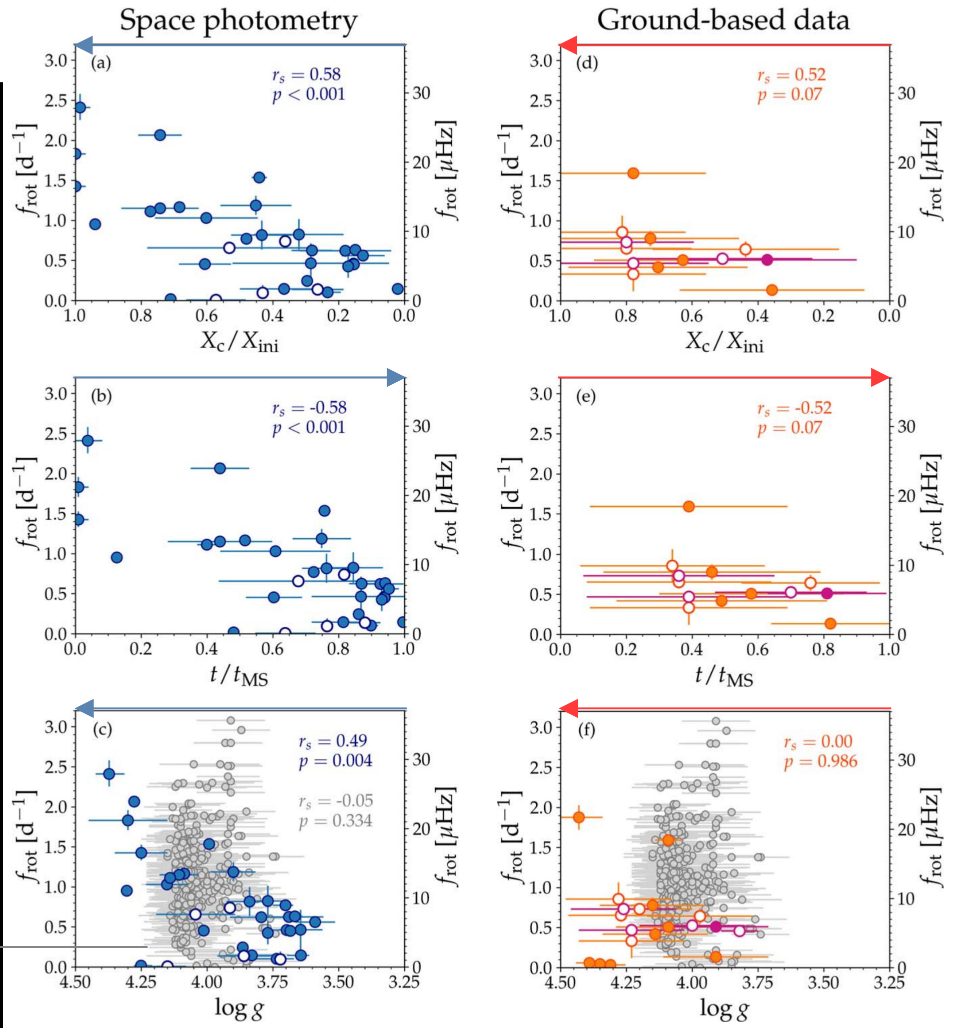

300 γDor stars
(Li et al., 2020, MNRAS 491, 3586)

Interior rotation profile

→ Pedersen, 2022, ApJ 940, 49

- 52 SPB stars for which
  - ✔ Internal rotation frequencies derived using g-mode oscillations
  - ✔ Unambiguous mode identification for at least one g-mode
  - ✔ Ages from X_c/X_{ini}, t/t_{MS} and/or log g

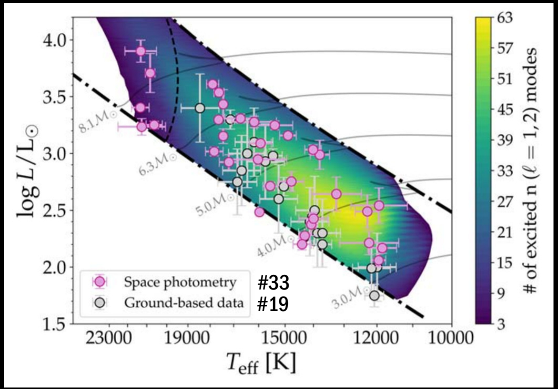

- Core rotation decreases with age
- Evidence for angular momentum transport
  - ✔ No angular momentum transport (no AM transport)
  - ✔ Most efficient angular momentum transport (solid body rotation)

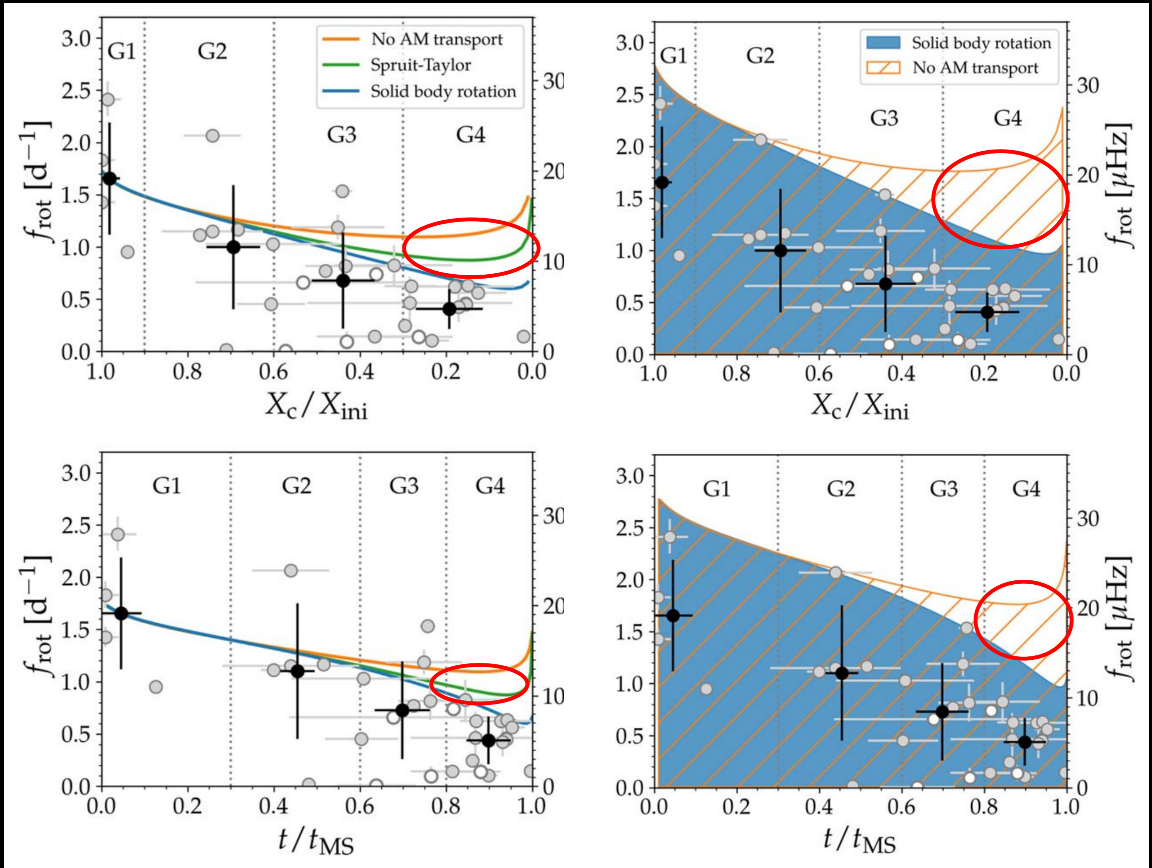

Scaled to average of G1

Scaled to individual stars

Interior rotation profile

→ Pedersen, 2022, ApJ 940, 49

- 52 SPB stars for which
  - ✔ Internal rotation frequencies derived using g-mode oscillations
  - ✔ Unambiguous mode identification for at least one g-mode
  - ✔ Ages from X_c/X_{ini}, t/t_{MS} and/or log g

Talk Bowman: "Asteroseismology reveals a unique anchor point for calibrating interior rotation, mixing and angular momentum transport in massive stars"

Talk Mombarg: "Testing the theory of angular momentum transport on the main sequence"

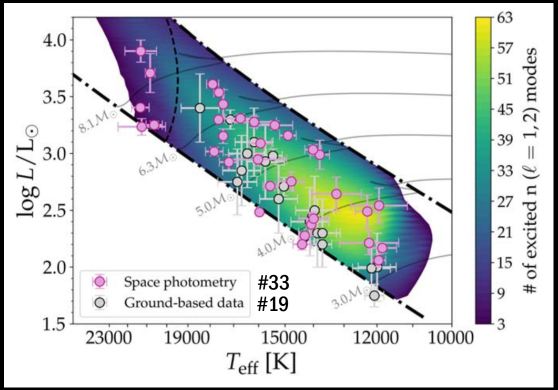

- Core rotation decreases with age
- Evidence for angular momentum transport
  - ✔ Rotationally split p-modes
  - ✔ Detection of more than one spacing pattern
  - ✔ Rotational spot modulation

} Search for differential rotation →

βCep stars:
- HD129929 (Aerts et al., 2003, Science 300, 1926)
- ν Eri (Dziembowksi & Pamyatnykh, 2008, MNRAS, 385, 2061)
- 12 Lac (Dziembowksi & Pamyatnykh, 2008, MNRAS, 385, 2061)
- HD192575 (Burssens et al., 2021, Posters from TSC2, 75)

SPB stars:
- KIC10526294 (Triana et al., 2015, ApJ 810, 16)
- HD201433 (Kallinger et al., 2017,A&A 603, A13)

Interior temperature profile

→ Michielsen et al., 2021, A&A 650, A175

- Investigated the thermal and chemical structure in the near-core region of stars with a convective core by means of gravito-inertial modes

→ Talk Michielsen: "Observational probing of core masses and thermal structures with gravity modes"

Tidal forces

→ **V453 Cygni** (Southworth et al., 2020, MNRAS 497, L19)

- Eclipsing binary consisting of B0.4IV and B0.7IV components (orbital period 3.89 days, slightly eccentric ~0.025, apsidal motion with period of 72 years)
- TESS (two sectors; 2-min cadence): 9 significant frequencies ⟹ at least one component with βCep pulsations

Fundamental p-mode frequency of primary and secondary component

Stochastic low-frequency variability?

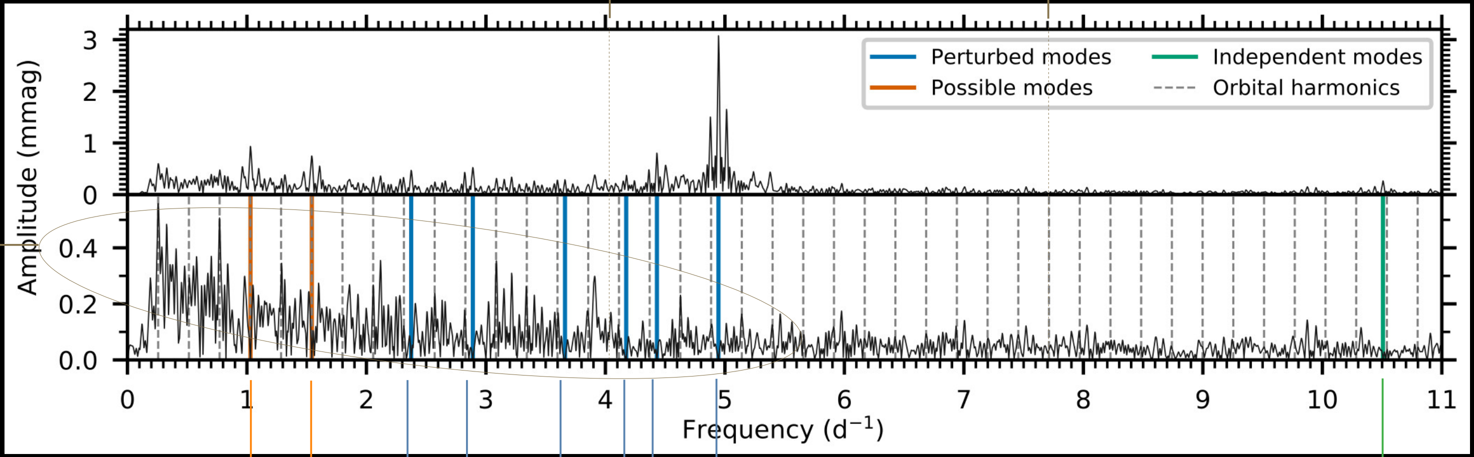

Tidally induced?
Imperfect binary model?

Quasi-constant offset of 0.06 d-1
from harmonics orbital frequency
⟹ Tidally perturbed pulsations!

No combination frequencies
Independent p-mode?

Tidal forces

→ V453 Cygni (Southworth et al., 2020, MNRAS 497, L19)

→ MACHO 80.7443.1718 (Kołaczek-Szymański et al., 2022, A&A 659, A47)

- Eccentric ellipsoidal variable (heartbeat star) consisting of blue supergiant and late O-type dwarf (orbital period 32.83 days, large eccentricity ~0.51) in LMC
- TESS (two seasons; 30-min cadence) + ground-based photometry (time base of 30 years): five tidally excited oscillations (TEO)

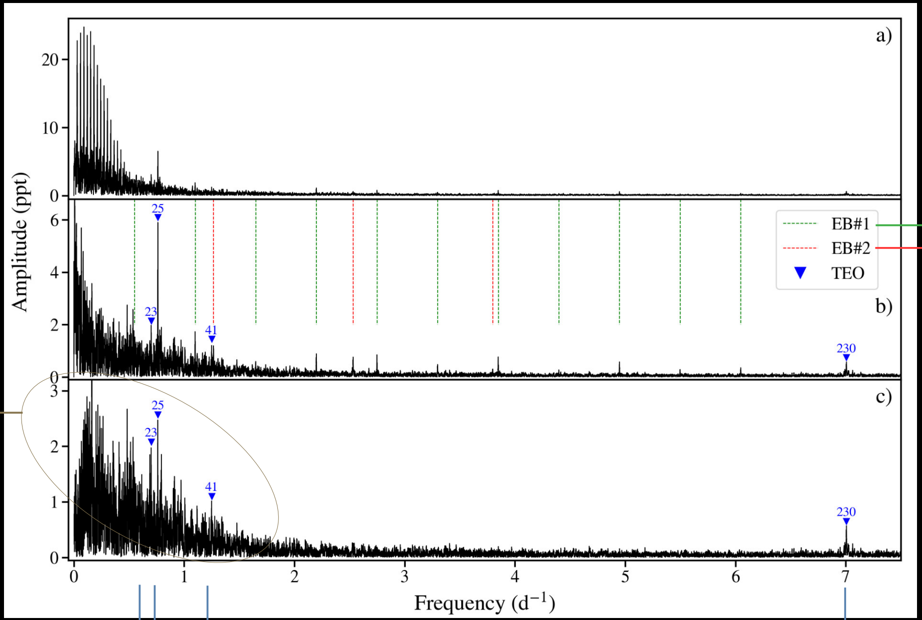

Nearby eclipsing binaries

Stochastic low-frequency variability

Tidally excited g-modes

Strongly non-adiabatic p-mode?
Strange mode?

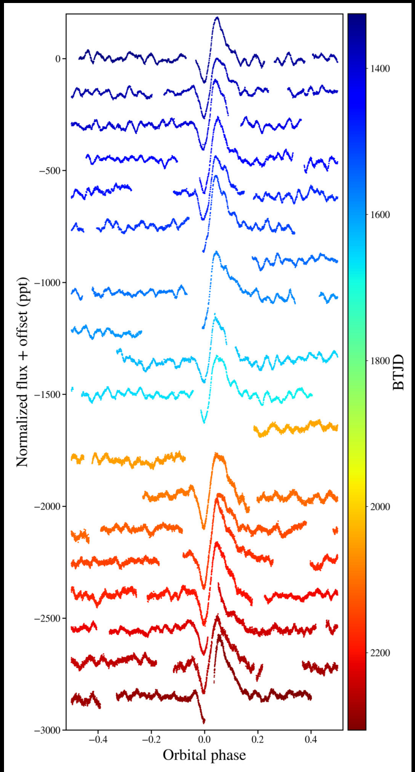

Tidal forces

→ V453 Cygni (Southworth et al., 2020, MNRAS 497, L19)

→ MACHO 80.7443.1718 (Kołaczek-Szymański et al., 2022, A&A 659, A47)

- Eccentric ellipsoidal variable (heartbeat star) consisting of blue supergiant and late O-type dwarf (orbital period 32.83 days, large eccentricity ~0.51) in LMC
- TESS (two seasons; 30-min cadence) + ground-based photometry (time base of 30 years): five tidally excited oscillations (TEO)

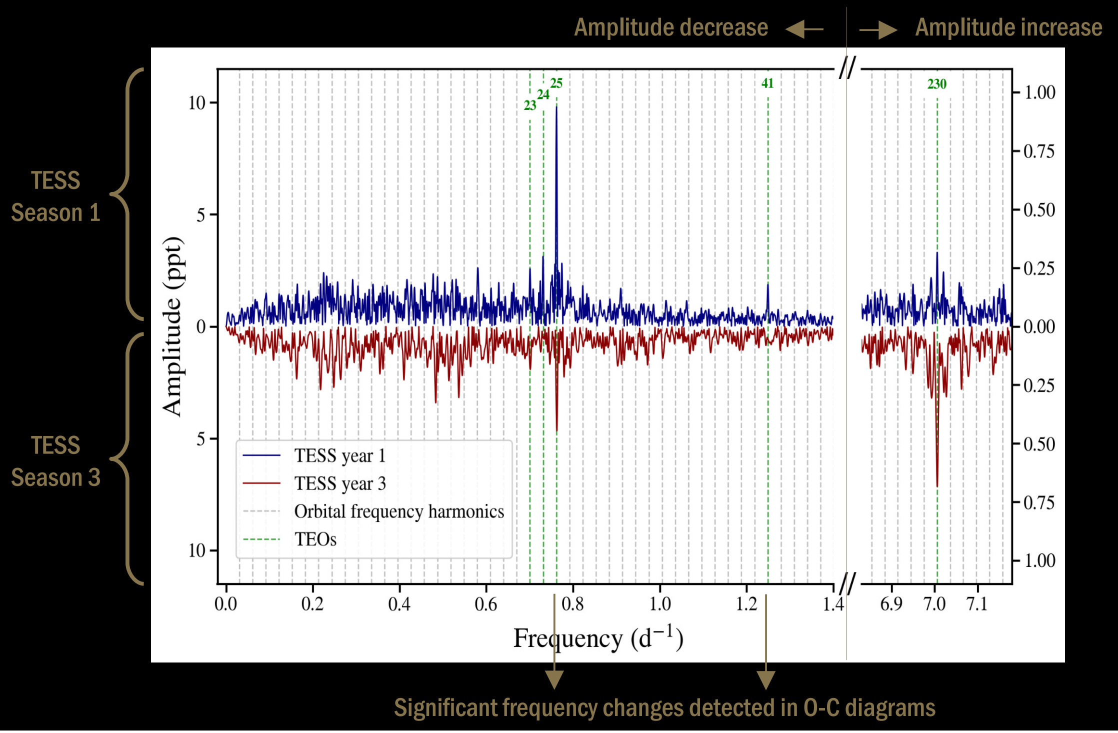

Amplitude and frequency changes for tidally excited oscillations

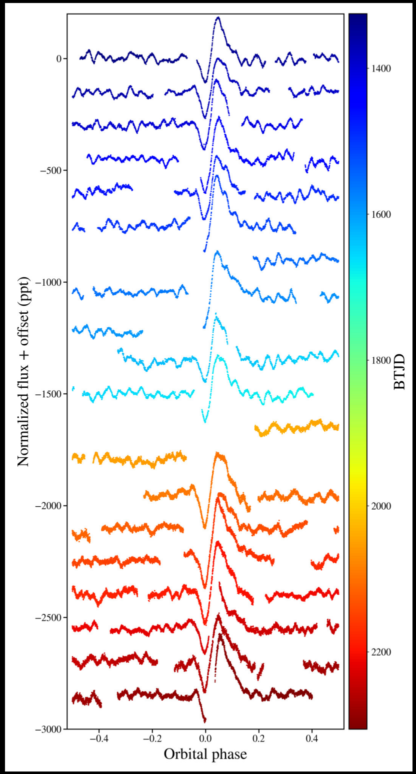

Tidal forces

→ V453 Cygni (Southworth et al., 2020, MNRAS 497, L19)

→ MACHO 80.7443.1718 (Kołaczek-Szymański et al., 2022, A&A 659, A47)

Poster 24 Szewczuk: “CW Cephei - the binary B-type pulsator”
Poster 41 Handler: “Tidally tilted pulsators: newsflash”
Poster 44 Eze: “Photometric sample of early B-type pulsators in eclipsing binaries observed with TESS”
Poster e2 Rocha: “Study of Be Stars in Binary Systems Observed with TESS”

Magnetic fields

→ Effects of magnetic field on asteroseismic diagnostics of pulsating stars

- Magnetic multiplets (Shibahashi & Aerts, 2000, ApJ 531, L143)
- Period spacings (Prat et al., 2020, A&A 636, A100)
- Inhibition of mixing ⇒ no overshooting (Briquet et al., 2016, A&A 587, A126)

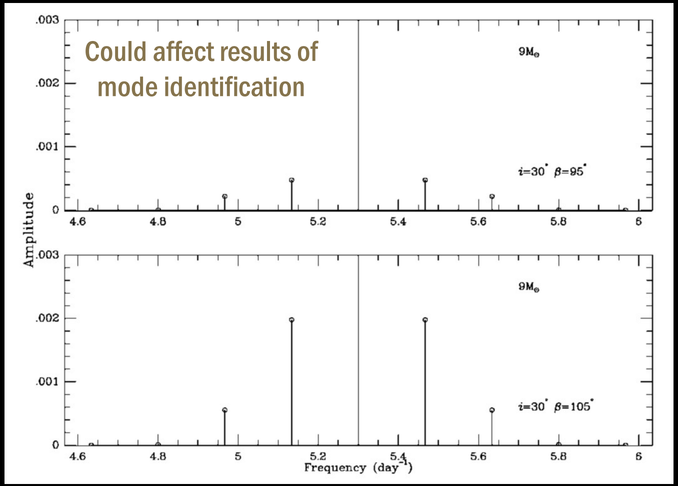

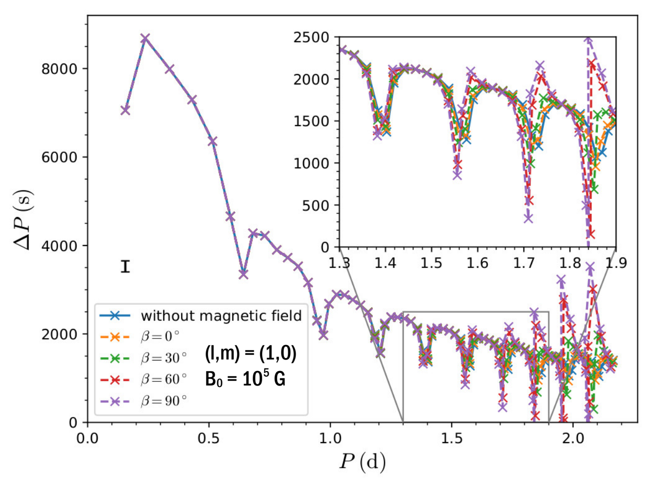

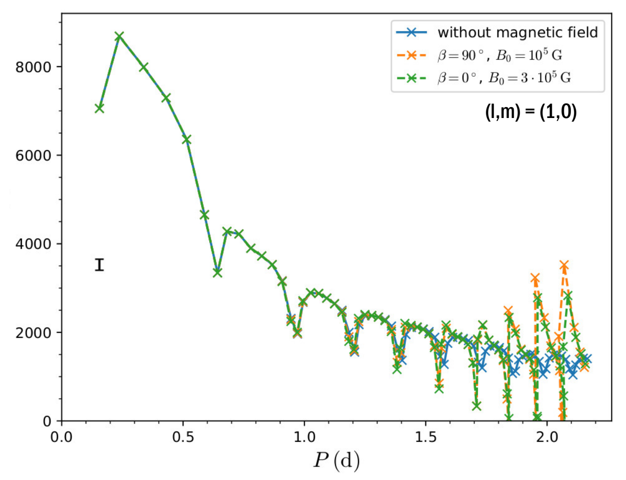

Magneto-asteroseismology

✔ Ground-based	β Cep	(Shibahashi & Aerts, 2000, ApJ 531, L143)
	ζ Cas	(Briquet et al., 2016, A&A 587, A126)
	V2052 Oph	(Briquet et al., 2012, MNRAS 427, 483)
✔ CoRoT	HD43317	(Buysschaert et al., 2018, A&A 616, A148)
✔ K2	ι Lib	(Buysschaert et al., 2018, SF2A Conf., 369)

Magnetic fields

→ Overview of surveys to (1) discover new magnetic massive stars with spectropolarimetric observations
(2) improve the models of magnetic stars

- BOB — B Fields in OB Stars (Morel et al., 2014, Messenger 157, 27)
  - ✔ Southern OB stars
- BritePol — BRITE spectropolarimetric survey (Neiner et al., 2014, SF2A Conf, 505)
  - ✔ ~600 stars with V ≤ 4
- BinaMIcs — Binarity and Magnetic Interactions in various classes of stars (Alecian et al., 2015, IAUS 307, 330)
  - ✔ ~200 hot binary stars
- MiMeS — Magnetism in Massive Stars (Wade et al., 2016, MNRAS 456, 2)
  - ✔ ~550 massive stars
- LIFE — Large Impact of magnetic Fields on the Evolution of hot stars (Martin et al., 2018, MNRAS 475, 1521)
  - ✔ ~60 evolved hot stars
- MOBSTER — Magnetic OB[A] Stars with TESS: probing their Evolutionary and Rotational properties (David-Uraz et al., 2019, MNRAS 487, 304)
  - ✔ confirmed and candidate magnetic OBA stars that are observed with TESS

Detected for ~10% of B stars

Talk David-Uraz: “Variability characteristics of OBA stars: how to find magnetic needles in a large data haystack”
Talk Vanlaer: “Asteroseismic constraints on the internal magnetic field of the TESS β Cephei pulsator HD 192575”
Poster 48 Berry: “Electron scattering emission in the light curves of CM stars observed with TESS and K2”
Poster e4 Keszthelyi: “Evolutionary and Population Synthesis Models of Magnetic Massive Stars”

Stochastic Low-Frequency Variability (SLFV)

→ Observations of SLFV (red noise excess at low frequencies)

✔ Blomme et al., 2011, A&A 533, A4 → HD46223, HD46150 & HD4696 (O stars)

CoRoT

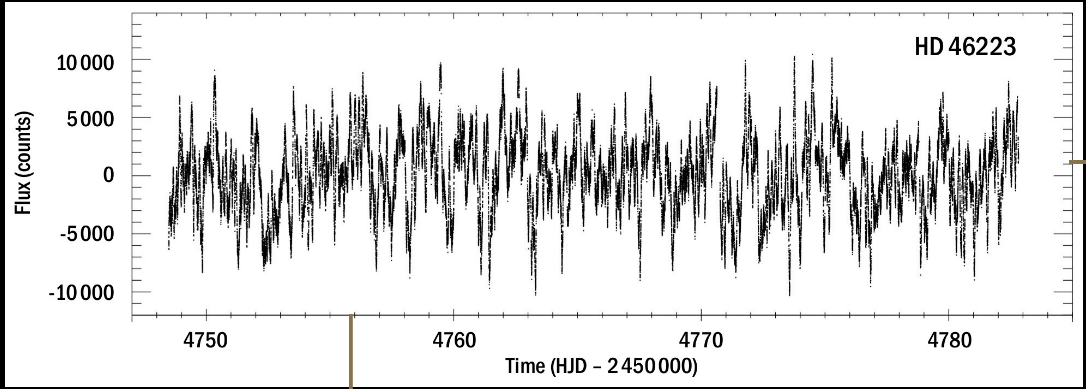

Time-dependent frequency analysis (sliding window)

Short-lived variability

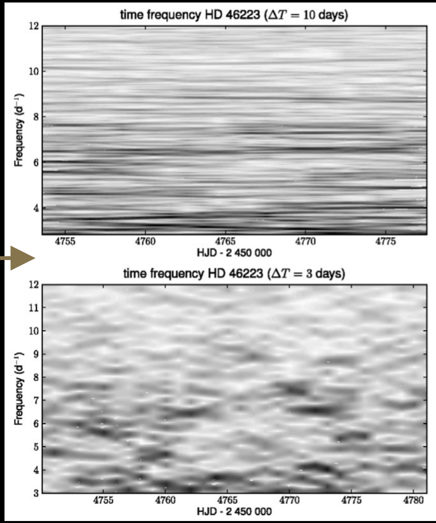

Stochastic excitation

Lomb-Scargle periodogram

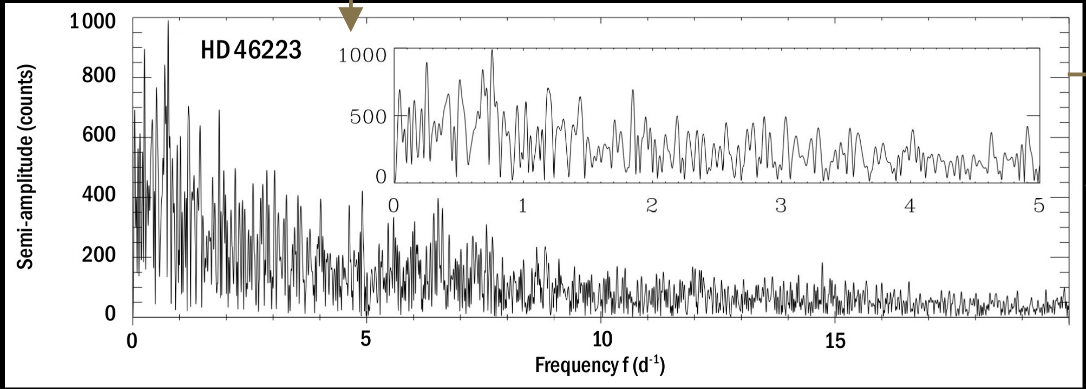

Semi-Lorentzian function

$$\alpha(f) = \frac{\alpha_0}{1 + (2\pi\tau_{char}f)^{\gamma}}$$

with

- α_0 amplitude as $f \rightarrow 0$
- τ_{char} characteristic timescale on which red noise is correlated
- γ steepness of amplitude spectrum

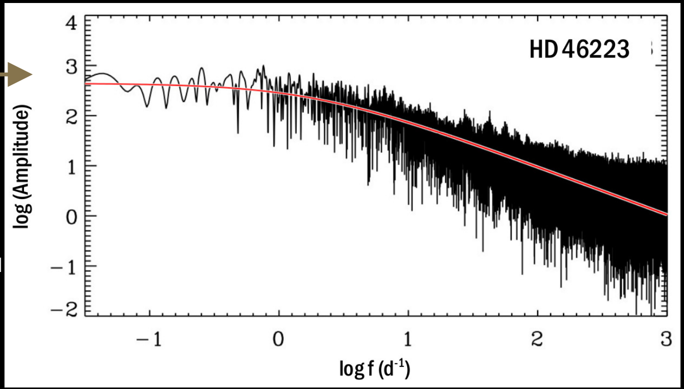

Stochastic Low-Frequency Variability (SLFV)

→ Observations of SLFV (red noise excess at low frequencies)

✔	Blomme et al., 2011, A&A 533, A4	→ HD46223, HD46150 & HD4696 (O stars)	CoRoT
✔	Tkachenko et al., 2014, MNRAS 438, 3093	→ primary of massive binary V380 Cyg (B star)	Kepler + spectra
✔	Aerts et al., 2017, A&A 602, A32	→ HD188209 (O9.5 Iab blue supergiant)	Kepler + spectra
✔	Simón-Díaz et al., 2018, A&A 612, A40	→ HD2905 (early-B supergiant)	spectra
✔	Bowman et al., 2019, A&A 621, A135	→ 35 OBAF stars	CoRoT
✔	Bowman et al., 2019, NatAs 3, 760	→ 114 ecliptic OB stars & 53 LMC OB stars	K2 + TESS
✔	Dorn-Wallenstein et al., 2019, AJ 878, 155	→ 6 LMC yellow supergiants & 2 LMC luminous blue variables	TESS
✔	Bowman et al., 2020, A&A 640, A36	→ 70 OB stars	TESS + spectra
✔	Dorn-Wallenstein et al., 2020, AJ 902, 24	→ 28 LMC yellow supergiants & 48 Galactic red supergiants	TESS
✔	Rauw et al., 2019, A&A 621, A15	→ HD149404 (massive post-Roche Lobe overflow system)	BRITE
✔	Nasé et al., 2021, MNRAS 502, 5038	→ 26 Wolf-Rayet stars & 8 luninous blue variables	TESS
✔	Lenoir-Craig et al., 2022, AJ 925, 79	→ 50 Galactic Wolf-Rayet stars	BRITE
✔	Elliot et al., 2022, MNRAS 509, 4246	→ P Cygni (luminous blue variable)	BRITE
✔	Bowman et al., 2022, A&A 668, A134	→ 30 OB stars	CoRoT
✔	Kołaczek-Szymański et al., A&A 659, A47	→ MACHO 80.7443.1718 (blue supergiant + late O-type dwarf)	TESS
✔	Dorn-Wallenstein et al., 2022, AJ 940, 27	→ 101 LMC and 25 SMC cool supergiants	TESS

Feature observed for many different types of massive stars!

Stochastic Low-Frequency Variability (SLFV)

→ Characterisation of SLFV (red noise excess at low frequencies)

- Amplitude spectrum fitting (frequency domain)
  - ✔ Semi-Lorentzian function
    - ➔ α_0 characteristic amplitude as frequency ⟶ 0
    - ➔ $\tau_{char} = 1/\nu_{char}$ characteristic timescale on which red noise is correlated
    - ➔ γ steepness of amplitude spectrum
    - ➔ α_w frequency independent noise term (white noise)
- Gaussian process regression (time domain)
  - ✔ Damped simple harmonic oscillator
    - ➔ σ_A characteristic amplitude
    - ➔ $\rho_{char} = 2\pi/\omega_0$ characteristic variability timescale
    - ➔ τ_{damp} characteristic damping timescale
    - ➔ C_{jitter} jitter term to emulate uncorrelated noise in the observations
    - ➔ Q quality factor (more damping if low value)

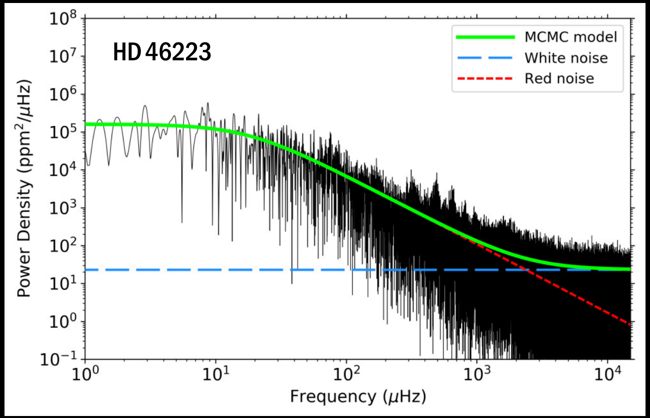

Bowman et al., 2019, A&A 621, A135

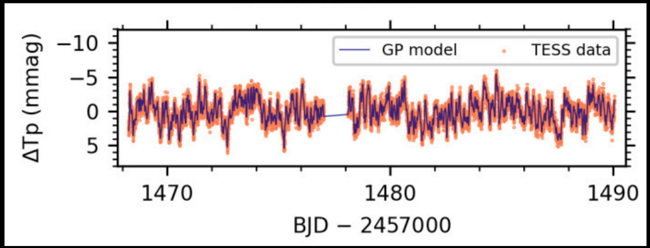

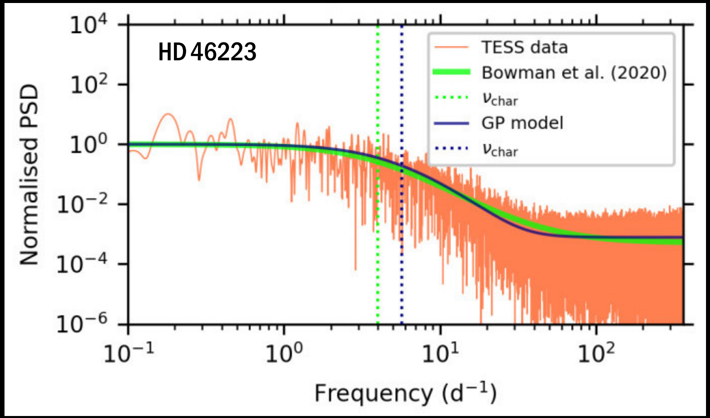

Bowman et al., 2022, A&A 668, A134

Stochastic Low-Frequency Variability (SLFV)

→ Characterisation of SLFV (red noise excess at low frequencies)

➢ Amplitude spectrum fitting (frequency domain)

✔ Semi-Lorentzian function

- ➔ α_0 characteristic amplitude as frequency ⟶ 0
- ➔ $\tau_{char} = 1/\nu_{char}$ characteristic timescale on which red noise is correlated
- ➔ γ steepness of amplitude spectrum
- ➔ α_w frequency independent noise term (white noise)

➢ Gaussian process regression (time domain)

✔ Damped simple harmonic oscillator

- ➔ σ_A characteristic amplitude
- ➔ $\rho_{char} = 2\pi/\omega_0$ characteristic variability timescale
- ➔ τ_{damp} characteristic damping timescale
- ➔ C_{jitter} jitter term to emulate uncorrelated noise in the observations
- ➔ Q quality factor (more damping if low value)

"yellow subgroup":
- Low ν_{char} + high α_0/σ_A + low ν_{damp}
- Higher mass
- More evolved (closer to TAMS)
- Less stochastic (high Q value)

"blue subgroup":
- High ν_{char} + low α_0/σ_A + high ν_{damp}
- Less evolved (closer to ZAMS)
- More stochastic (low Q values)

ν_{char} probes mass, age and degree of coherency

Bowman et al., 2022, A&A 668, A134

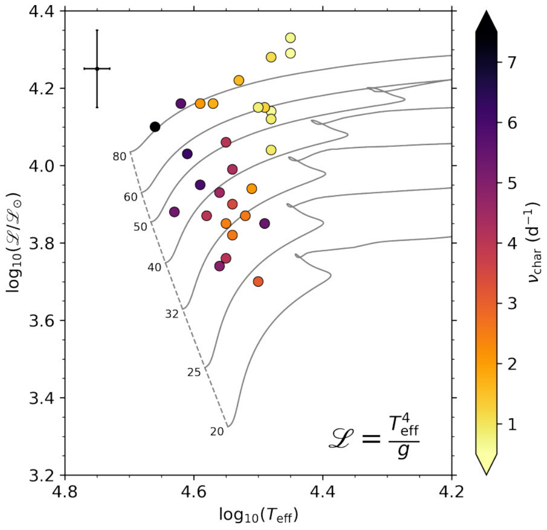

Bowman et al., 2022, A&A 668, A134

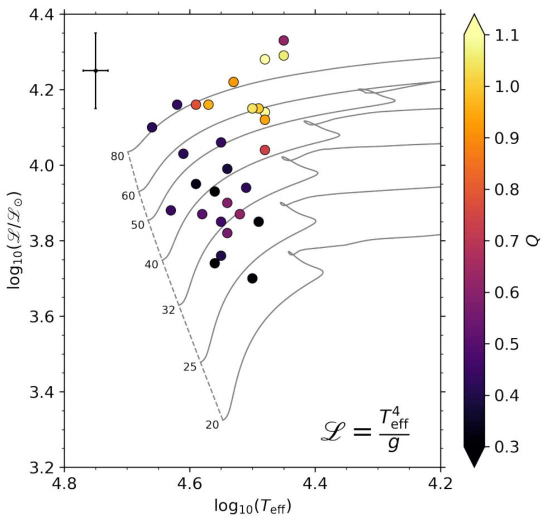

Stochastic Low-Frequency Variability (SLFV)

→ Interpretation of SLFV

- Surface granulations
  - ✔ Photometric amplitude is expected to scale inversely with number of convective granules on surface
  - ✔ Timescale is expected to scale with the ratio of the size and the sound speed of a granule
  - ✔ Tight correlation between ν_{gran} and stellar parameters for pulsating solar-type and red giant stars

(Kallinger et al., 2014, A&A 570, A41)

ν_{char} order of magnitude smaller than predicted ν_{gran} for majority of stars

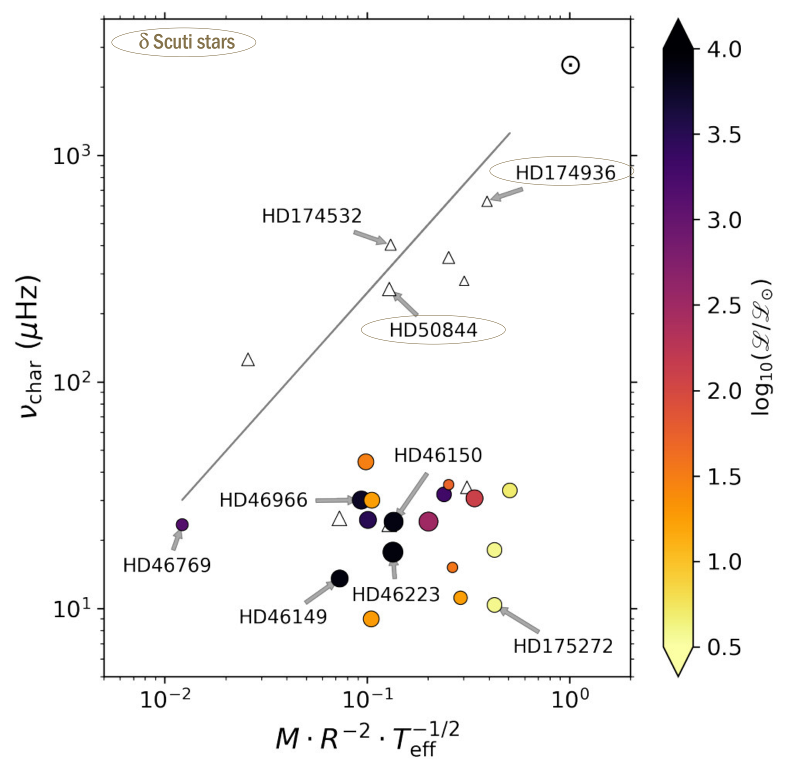

Bowman et al., 2019, A&A 621, A135

Stochastic Low-Frequency Variability (SLFV)

→ Interpretation of SLFV

- Surface granulations
- Internal Gravity Waves (IGWs)
  - ✔ Travelling waves that are stochastically excited at the interface of a convective region and a stably stratified zone
    - ➔ turbulent core convection
    - ➔ turbulent pressure fluctuations in subsurface convective zones in outer envelope (Fe-opacity peak converction zone)
  - ✔ Propagate and dissipate within radiative regions

Core excitation

pros
- ✔ Natural explanation for macroturbulent broadening (g-modes have high amplitude in wings) (e.g. Aerts et al., 2017, A&A 602, A32; Simón-Díaz et al., 2018, A&A 612, A40)
- ✔ Natural explanation for angular momentum transport (e.g. Rogers et al., 2013, AJ 772, 21)
- ✔ Most observations compatible with $0.8 \lesssim \gamma \lesssim 3.5$ predicted from simulations (e.g. Edelmann et al., 2019, ApJ 876, 4; Ratnasignam et al., 2023, A&A 674, A134)

cons
- ✔ Dominant broad peaks compatible with standing g-modes (stochastially excited through resonance) (Lecoanet et al., 2019, AJ 886, L15; Lecoanet et al., 2021, MNRAS 508, 132)
- ✔ Photometric variability is orders of magnitude lower than observed red noise (Anders et al., 2023, NatAs, accepted)

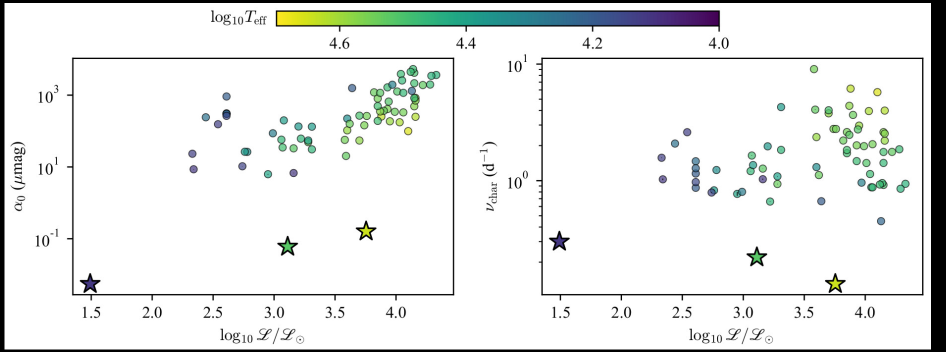

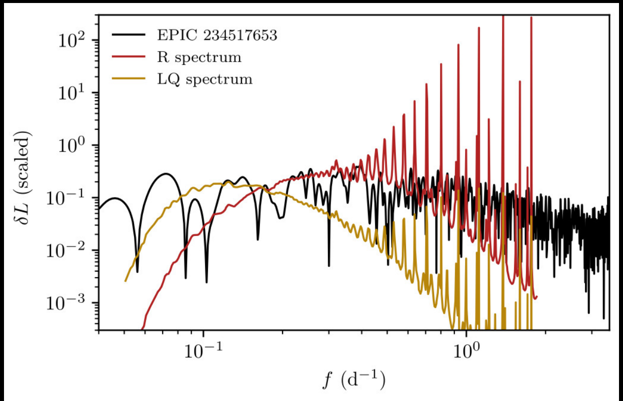

KSB - ORB

Stochastic Low-Frequency Variability (SLFV)

→ Interpretation of SLFV

- Surface granulations
- Internal Gravity Waves (IGWs)
  - ✔ Travelling waves that are stochastically excited at the interface of a convective region and a stably stratified zone
    - ➔ turbulent core convection
    - ➔ turbulent pressure fluctuations in subsurface convective zones in outer envelope (Fe-opacity peak converction zone)
  - ✔ Propagate and dissipate within radiative regions

Core excitation

pros

- ✔ Natural explanation for macroturbulent broadening (g-modes have high amplitude in wings) (e.g. Aerts et al., 2017, A&A 602, A32; Simón-Díaz et al., 2018, A&A 612, A40)
- ✔ Natural explanation for angular momentum transport (e.g. Rogers et al., 2013, AJ 772, 21)
- ✔ Most observations compatible with $0.8 \lesssim \gamma \lesssim 3.5$ predicted from simulations (e.g. Edelmann et al., 2019, ApJ 876, 4; Ratnasignam et al., 2023, A&A 674, A134)

cons

- ✔ Dominant broad peaks compatible with standing g-modes (stochastially excited through resonance) (Lecoanet et al., 2019, AJ 886, L15; Lecoanet et al., 2021, MNRAS 508, 132)
- ✔ Photometric variability is orders of magnitude lower than observed red noise (Anders et al., 2023, NatAs, accepted)

Subsurface excitation

pros

- ✔ Calculation wave transfer function (Lecoanet et al., 2019, AJ 886, L15; Lecoanet et al., 2021, MNRAS 508, 132)
- ✔ 1D nonrotating stellar evolution calculations (Cantiello et al., 2021, AJ 915, 112)
- ✔ 3D radiation hydrodynamical simulations of two 35 $M_\odot$ star envelopes (Schultz et al., 2022, AJ 924, L11)

Stochastic Low-Frequency Variability (SLFV)

→ Interpretation of SLFV

- Surface granulations
- Internal Gravity Waves (IGWs)
- Wind-driven processes
  - ✔ Clumpy, aspherical, and inhomogeous stellar wind
    Krtička & Feldmeier, 2021, A&A 648, A79
  - ✔ TESS data of 116 O-type stars and 18 B-type supergiants with purely stochastic variability
  - ✔ Signatures of line-driven wind instability in photometric data
    - ➔ a knee in the power spectrum of magnitude fluctuations, which appears due to engulfment of small-scale structure by larger structures
    - ➔ a negative skewness of the distribution of fluctuations, which is the result of spatial dominance of rarefied regions

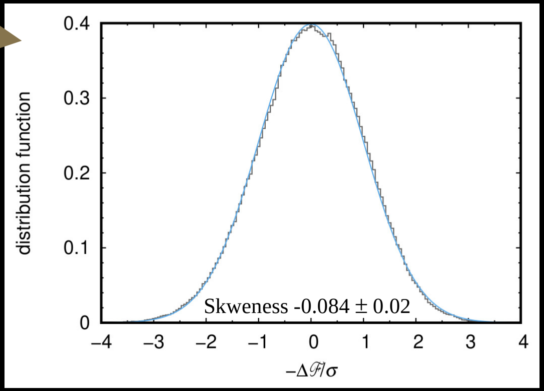

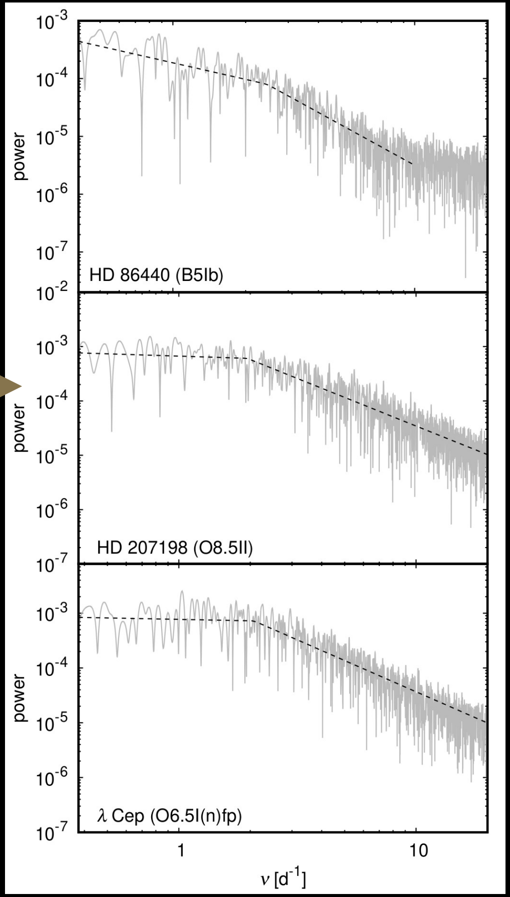

Observations: e.g. Aerts et al., 2018, MNRAS 476, 1234; Ramiaramanantsoa et al., 2018, MNRAS 473, 5532
Modeling: e.g. Krtička & Feldmeier, 2018, A&A 617, A121; Krtička & Feldmeier, 2021, A&A 648, A79

Be stars

~20% of non-supergiant B stars

- Balmer lines in emission (circumstallar accretion disk)
- Rapid rotators

→ Structure of frequency spectra

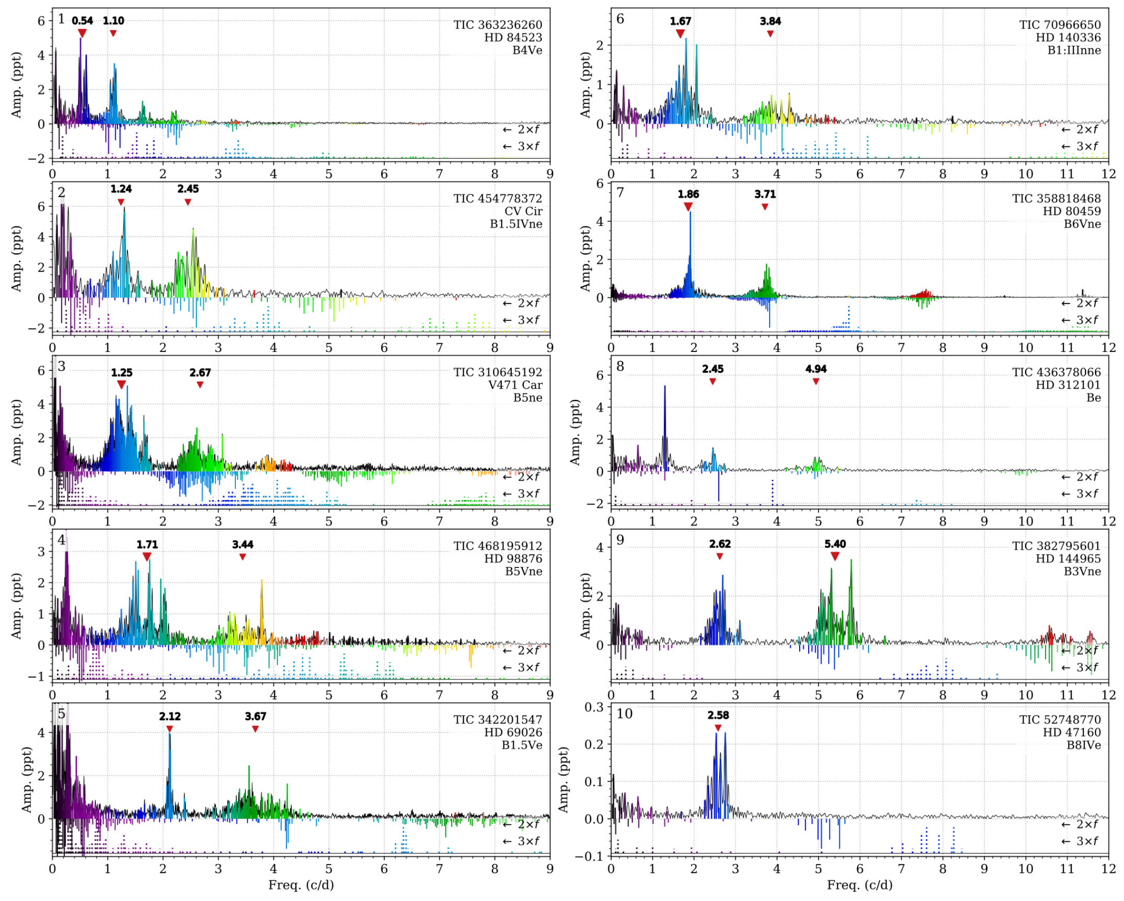

Labadie-Bartz et al., 2022, AJ 163, 226

Be stars

~20% of non-supergiant B stars

- Balmer lines in emission (circumstallar accretion disk)
- Rapid rotators

→ Structure of frequency spectra

→ Variable frequencies and amplitudes

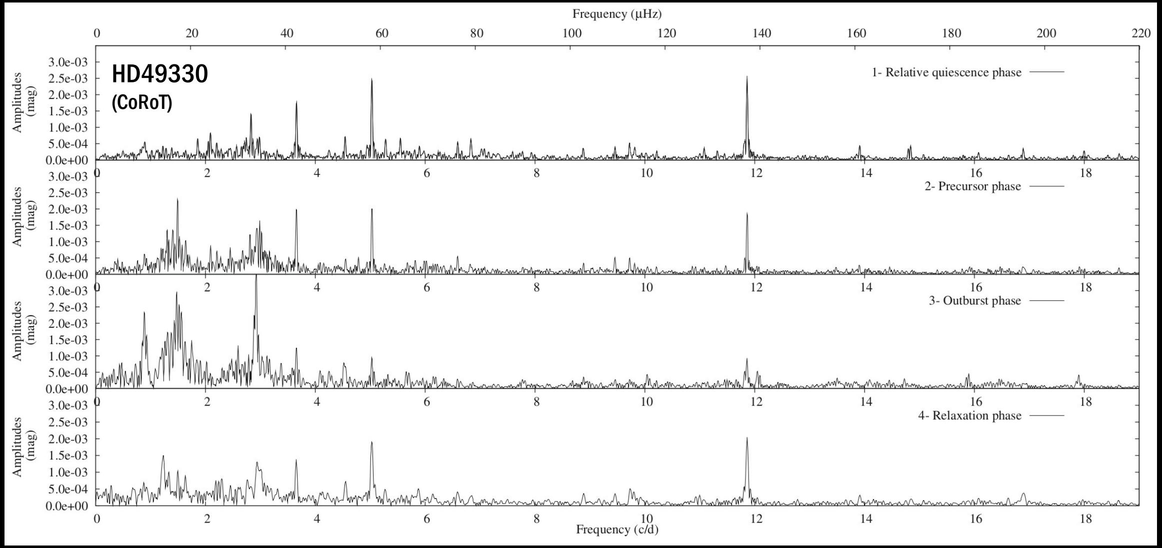

Huat et al., 2009, A&A 506, 95

Baade et al., 2018, A&A 610, A70

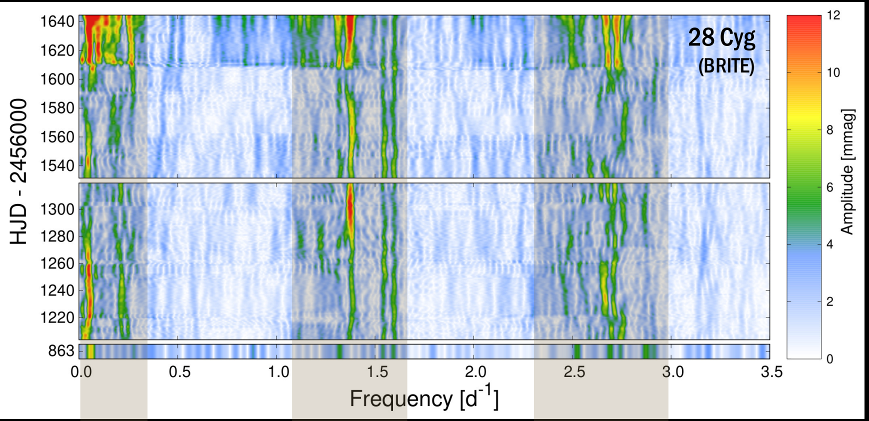

Poster e2 Rocha: "Study of Be Stars in Binary Systems Observed with TESS"

Poster e23 Labadie-Bartz: "TESS photometry + simultaneous spectroscopy of classical Be stars: pulsation, mass ejection, and disc formation"

g_2 Harmonics and sum frequencies

g_1 g mode pulsations

Štefl frequency (exophotospheric; due to inhomogeneous distribution of recently ejected material orbiting the star) → very large amplitude

g_0 Difference frequencies (difference of g modes with amplitude larger than the sum of the inividuel g modes) → triggers mass loss episodes

OB-type stars

Convective core
Radiative envelope

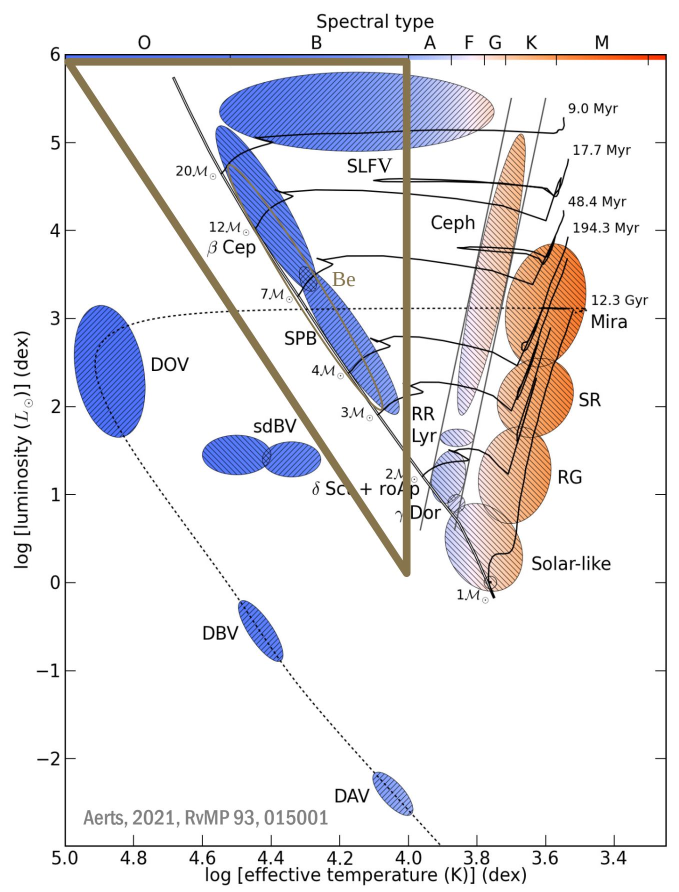

- → **β Cephei stars** (βCep)
  - Low order p and g modes with periods of few hours
- → **Slowly Pulsating B stars** (SPB)
  - High order g modes with periods of several hours to few days

} Hybrids!

- → **Stochastic low-frequency variability** (SLFV)
  - α Cygny stars
  - Fast Yellow Pulsating Supergiants (?) → Talk Pederson: "Identifying contaminating sources in TESS light curves"
- → **Be stars** (Be)
  - Pulsations
- → **Maia variables (?)**
  - → Talk Handler: "Maia variables - fact or fiction?"

Excitation mechanisms at play

- Opacity mechanism operating in Z bump
- Stochastic excitation
- Non-linear mode excitation
- Rotation
- Tidal excitation

Influencing factors

- Opacities
- Interior mixing profile
- Interior rotation profile
- Interior temperature profile
- Tidal forces
- Magnetic fields
- Mass loss
- Stellar wind

Thank you!

Announcement

The third LAMOST-Kepler/TESS workshop

Synergies between ground-based spectroscopic surveys and space-based photometric missions

Date: May 28-31, 2024

City: Beijing of China

Host: Institute For Frontiers in Astronomy and Astrophysics (IFAA) of Beijing Normal University (BNU)